

CONSTRAINTS ON LORENTZ INVARIANCE VIOLATION WITH GAMMA-RAY BURSTS VIA A MARKOV CHAIN MONTE CARLO APPROACH

YU PAN^{1,2}, YUNGUI GONG³, SHUO CAO², HE GAO⁴ AND ZONG-HONG ZHU^{2*}

Draft version April 9, 2021

ABSTRACT

In quantum theory of gravity, we expect the Lorentz Invariance Violation (LIV) and the modification of the dispersion relation between energy and momentum for photons. The effect of the energy-dependent velocity due to the modified dispersion relation for photons was studied in the standard cosmological context by using a sample of Gamma Ray Bursts (GRBs). In this paper we mainly discuss the possible LIV effect by using different cosmological models for the accelerating universe. Due to the degeneracies among model parameters, the GRBs' time delay data are combined with the cosmic microwave background data from the Planck first year release, the baryon acoustic oscillation data at six different redshifts, as well as Union2 type Ia supernovae data, to constrain both the model parameters and the LIV effect. We find no evidence of LIV.

Keywords: gravitation— (stars:) gamma-ray burst: general— (cosmology:) dark energy

1. INTRODUCTION

Above the Planck energy scale E_{Pl} , we expect a quantum theory of gravity in place of Einstein's general relativity. The quantization of space-time will lead to the modification of the dispersion relation between energy and momentum of a particle with mass m and the breakdown of Lorentz invariance. In some quantum gravity models, the consequence of the Lorentz Invariance Violation (LIV) is the energy dependence of the speed of light in vacuum (Amelino-Camelia et al. 1998, 2001). In these scenarios, the energy dependent velocity of light is $v = c(1 - \xi E/E_{\text{QG}})$ with effective quantum gravity energy scale E_{QG} , the speed of high energy photons is slower, and low energy photons will reach us earlier. Therefore, the measurement of the light speed in vacuum can be used to study the LIV effect.

In the past years, both astrophysics and particle physics' experiments have been proposed to test the LIV and quantum gravity effects (Mattingly et al. 2005; Sarkar et al. 2002; Amelino-Camelia. 2013). Because photons with different energy will reach us at different time, and the energy of Gamma-Ray Bursts (GRBs) which are the most luminous explosions in the universe with short duration ranges from KeV to GeV, GRBs with intense bursts of γ -ray photons from cosmological distances are proposed to measure the difference of the arrival time of photons with different energy (Amelino-Camelia et al. 1998, 2002; Kowalski-Glikman & Nowak 2002). GRBs were also used to constrain LIV theories (Ellis et al. 2003, 2006; Rodriguez Martínez & Piran 2006; Jacob et al. 2007). Biller et al. (1999) used the data for a TeV γ -ray flare

coming from the active galaxy Markarian 421 to set a bound on the energy scale of quantum gravity as $E_{\text{QG}} > 6 \times 10^{16}$ GeV. Abdo et al. (2009a) used GRB 090510 to study the LIV effect and get $E_{\text{QG}} > 1.2E_{\text{Pl}}$, the energy scale of quantum gravity was found to be $E_{\text{QG}} > 1.3 \times 10^{18}$ GeV by using GRB 080916C. The LIV effects due to extra dimensions can also be constrained by GRBs (Baukh et al. 2007). Experiments with cold atoms were also proposed to constrain the modified dispersion relation due to quantum gravity (Amelino-Camelia et al. 2009).

In order to measure the LIV, statistical and possible systematic uncertainties must be minimized. For this purpose, Ellis et al. (2003, 2006) developed a method to analyze samples of GRBs with different redshifts and energy bands. The technique has the advantage of extracting time-dependent features from the signals of many GRBs. In the analysis (Ellis et al. 2003), they used both the BATSE and OSSE data from the Compton Gamma Ray Observatory⁵. By adding larger samples of GRBs with known redshifts from HETE⁶ and SWIFT⁷, the observed time delay was formulated in terms of linear regression where the intercept denotes intrinsic time delay and the linear term denotes LIV effect (Ellis et al. 2008; Jacob et al. 2008). By using the concordance Λ CDM model with $\Omega_{\Lambda} = 0.7$, they found no strong evidence of LIV, and they obtained $E_{\text{QG}} \geq 1.4 \times 10^{16}$ GeV (Ellis et al. 2006).

Since the distances from the sources to the observer depend on cosmological models, the conclusions on the LIV and quantum gravity effect may be affected by the cosmological model used in the analysis. However, only the concordance Λ CDM scenario ($\Omega_{\Lambda} = 0.7$, $\Omega_m = 0.3$) was studied (Ellis et al. 2003). Therefore, it is necessary to consider other cosmological models. Recently Biesiada et al. (2009) studied the LIV by using the quintessence and Chaplygin Gas model and they found a

¹ College of Science, Chongqing University of Posts and Telecommunications, Chongqing 400065, China

² Department of Astronomy, Beijing Normal University, Beijing 100875, China; zhuzh@bnu.edu.cn

³ MOE Key Laboratory of Fundamental Quantities Measurement, School of Physics, Huazhong University of Science and Technology, Hubei 430074, China

⁴ Department of Astronomy and Astrophysics, Pennsylvania State University, 525 Davey Laboratory, University Park, PA 16802

⁵ <ftp://legacy.gsfc.nasa.gov/compton/data/batse/ascii/data/64ms/>

⁶ <http://space.mit.edu/HETE/Bursts/>

⁷ <http://swift.gsfc.nasa.gov/docs/swift/archive/>

weak evidence of LIV. In their analysis, the degeneracies among model parameters were neglected, as they were taken as fixed values. In this paper we mainly discuss the possible LIV by using different cosmological models which explain the present cosmic acceleration. Compared with the previous work, in addition to the relevant parameters quantifying LIV, the cosmological parameters are also treated as free parameters. We adopt the Markov Chain Monte Carlo (MCMC) technique to constrain LIV and model parameters with the observational data. In order to derive tighter constraints on the model parameters, we combine the time delay data from GRBs with the cosmic microwave background (CMB) data from the Planck first year release (Ade et al. 2014; Wang et al. 2013), the baryon acoustic oscillation (BAO) data (Blake et al. 2011; Beutler et al. 2011; Gong et al. 2014; Percival et al. 2010), and the 557 Union2 SNeIa data (Amanullah et al. 2010). This paper is organized as follows: we introduce the LIV in section II. The GRBs' time delay and other observational data are discussed in section III. The constraint results on LIV and cosmological parameters with different cosmological models are presented in section IV, and finally, the conclusions are drawn in section V.

2. THE LORENTZ INVARIANCE VIOLATION

The modified dispersion relation due to quantum gravity models can be parameterized as follows (Ellis et al. 2003; Biesiada et al. 2009)

$$E^2 - p^2 c^2 = \epsilon E^2 \left(\frac{E}{\xi_n E_{QG}} \right)^n, \quad (1)$$

where ξ_n is a dimensionless parameter, $\xi_1 = 1$, $\xi_2 = 10^{-7}$ (Jacob et al. 2007), $\epsilon = +1$, and the effective energy scale E_{QG} of quantum gravity is expected to be near the Planck scale. Because the LIV effects are small, (Ellis et al. 2008; Biesiada et al. 2009), we consider the $n = 1$ term only in this study.

Since the arrival time for photons with energy E is equal to (Jacob et al. 2007, 2008; Biesiada et al. 2007, 2009)

$$t_{LIV} = \int_0^z \left[1 + \frac{E}{E_{QG}}(1+z') \right] \frac{dz'}{H(z')}, \quad (2)$$

so the the arrival times of two photons with different energy will be different, and the difference in time for the energy difference ΔE is

$$\Delta t_{LIV} = \frac{\Delta E}{H_0 E_{QG}} \int_0^z \frac{(1+z') dz'}{h(z')}, \quad (3)$$

where the dimensionless Hubble parameter $h(z) = H(z)/H_0$, H_0 is the Hubble constant and $H(z)$ is the Hubble parameter at redshift z . In order to account for the unknown intrinsic time lags, we fit the measured time-lags by including a parameter b specified in the rest frame of the source. The arrival time delays are fitted by the formula $\Delta t_{obs} = \Delta t_{LIV} + b(1+z)$ (Ellis et al. 2006). Therefore, the simple linear fitting function is

$$\frac{\Delta t_{obs}}{1+z} = a_{LIV} K + b, \quad (4)$$

where the intercept represents the intrinsic time lags, the LIV effects are encoded in the slope $a_{LIV} =$

$\Delta E/(H_0 E_{QG})$ which is related to the scale of Lorentz violation (Jacob et al. 2008; Biesiada et al. 2007) and $K = (1+z)^{-1} \int_0^z dz'(1+z')/h(z')$ is related to the measurements of cosmic distances. The model dependence is through the function $K(z)$ which will be calculated for three popular cosmological models.

3. THE OBSERVATIONAL DATA

In this paper we use the BATSE data with 9 light curves whose time resolution is 64 ms and redshifts span from $z = 0.835$ to $z = 3.9$, the HETE data with 15 light curves whose time resolution is 164 ms and redshifts span from $z = 0.168$ to $z = 3.372$, and the SWIFT data with 11 light curves whose time resolution is 64 ms and redshifts span from $z = 0.258$ to $z = 6.29$, the data was shown in Table 1 of Ellis et al. (2006). So we use the data of time lags between different energy channels measured from the light curves of 35 GRBs with redshifts from $z = 0.168$ to $z = 6.29$ (Ellis et al. 2006). The spectral time lags are obtained from the light curves in the 115-320 keV energy band with respect to those in the lowest 25-55 keV energy band. To test the LIV effect, we apply the χ^2 statistics, here χ^2 is

$$\chi_{GRBs}^2 = \sum_{i=1}^{N_{GRBs}} \left[\frac{\Delta t_i - \Delta t_{obs}}{\sigma_i} \right]^2, \quad (5)$$

where Δt_i and Δt_{obs} respectively denote the theoretical and observational values of time delays of GRBs, and σ_i is the observational uncertainty.

In fitting the data, in addition to the slope a_{LIV} and the intercept b , we also need to fit the model parameters. In previous studies, the model parameters are fixed and the degeneracies among parameters are neglected. To account for the degeneracies among these parameters, it would be better to treat the model parameters as free parameters and estimate their nominal values from the observational data. With this aim, we combine the CMB data from the Planck first year release, the 557 Union2 SNeIa data, and the BAO data with the data of spectral time lags from GRBs to constrain the model parameters. Since we have at least four parameters to fit, we take the MCMC (Lewis et al. 2002) technique to constrain the model parameters.

For the 557 Union2 SNeIa data, the distance modulus $\mu(z)$ is measured at different redshifts, and the theoretical value of the distance modulus is

$$\mu = 5 \log \frac{d_L}{Mpc} + 25 = 5 \log_{10} H_0 d_L - \mu_0, \quad (6)$$

where $\mu_0 = 5 \log_{10} [H_0 / (100 \text{ km/s/Mpc})] - 42.38$, and the luminosity distance is $d_L = (1+z) H_0^{-1} \int_0^z dz'/E(z')$. To fit the 557 Union2 SNeIa data, we calculate

$$\chi_{SNe}^2 = \sum_{i=1}^N \frac{[\mu(z_i) - \mu_{obs}(z_i)]^2}{\sigma_{\mu i}^2}, \quad (7)$$

where $\mu(z_i)$ and $\mu_{obs}(z_i)$ are the theoretical and observed distance modulus for the SNeIa at redshift z_i . The $\sigma_{\mu i}$ is observational error. For the nuisance parameter H_0 , we marginalize it with a flat prior.

The BAO A data consist of the measurements of A at three redshifts $z = 0.44$, $z = 0.6$ and $z = 0.73$ from Wig-

Table 1

 The corresponding inverse covariance matrix of A .

Redshift slice	$0.2 < z < 0.6$	$0.4 < z < 0.8$	$0.6 < z < 1.0$
$0.2 < z < 0.6$	1040.3	-807.5	336.8
$0.4 < z < 0.8$		3720.3	-1551.9
$0.6 < z < 1.0$			2914.9

glZ dark energy survey (Blake et al. 2011; Gong et al. 2014), and the parameter A is defined as

$$A = \sqrt{\Omega_m} \frac{H_0 D_V(z)}{z}, \quad (8)$$

where the effective distance is given by (Eisenstein et al. 2005)

$$D_V(z) = \left[\frac{d_L^2(z)}{(1+z)^2} \frac{z}{E(z)} \right]^{1/3}. \quad (9)$$

The χ^2 value for this data set is

$$\chi_{\text{BAO1}}^2 = \Delta \mathbf{A}_{\text{BAO}}^T \mathbf{C}_{\text{BAO}}^{-1} \Delta \mathbf{A}_{\text{BAO}}, \quad (10)$$

where $\mathbf{C}_{\text{BAO}}^{-1}$ is the corresponding inverse covariance matrix (See Table 1).

In addition to the above A parameter, we also consider the BAO distance ratio d_z at $z = 0.2$ and $z = 0.35$ from SDSS data release 7 (DR7) galaxy sample (Percival et al. 2010) and $d_{0.106} = 0.336 \pm 0.015$ from the 6dFGS measurements (Beutler et al. 2011). The BAO distance ratio is

$$d_z = \frac{r_s(z_d)}{D_V(z)}, \quad (11)$$

where the comoving sound horizon is

$$r_s(z) = \int_z^\infty \frac{c_s(z) dz}{E(z)}, \quad (12)$$

the sound speed $c_s(z) = 1/\sqrt{3[1 + \bar{R}_b/(1+z)]}$, and $\bar{R}_b = 3\Omega_b h^2/(4 \times 2.469 \times 10^{-5})$. As usual, we fit the drag redshift z_d as follows (Eisenstein et al. 1998)

$$\begin{aligned} z_d &= \frac{1291(\Omega_m h^2)^{0.251}}{1 + 0.659(\Omega_m h^2)^{0.828}} [1 + b_1(\Omega_b h^2)^{b_2}], \\ b_1 &= 0.313(\Omega_m h^2)^{-0.419} [1 + 0.607(\Omega_m h^2)^{0.674}], \\ b_2 &= 0.238(\Omega_m h^2)^{0.223}. \end{aligned} \quad (13)$$

The χ^2 value of the BAO distance ratio is (Percival et al. 2010)

$$\chi_{\text{BAO2}}^2 = \Delta \mathbf{P}_{\text{BAO}}^T \mathbf{C}_{\text{BAO}}^{-1} \Delta \mathbf{P}_{\text{BAO}}, \quad (14)$$

where $\Delta \mathbf{P}_{\text{BAO}} = \mathbf{P}_{\text{th}} - \mathbf{P}_{\text{obs}}$, \mathbf{P}_{obs} is the observed distance ratio, and \mathbf{C}_{BAO} is the covariance matrix for the distance ratio. To use the BAO data, we minimize

$$\chi_{\text{BAO}}^2 = \chi_{\text{BAO1}}^2 + \chi_{\text{BAO2}}^2 + \frac{(d_{0.106} - 0.336)^2}{0.015^2}. \quad (15)$$

For the CMB measurement, we use the derived parameters including the acoustic scale l_a , the shift parameter R , and $\Omega_b h^2$ (Ade et al. 2014; Wang et al. 2013) from the Planck temperature measurements combined

Table 2

 The 1σ and 2σ constraints on a and b for different cosmological model.

Cosmological model	Regression coefficient a and intercept b
Λ CDM	$a = -0.017^{+0.0717, +0.1416}_{-0.0718, -0.1415}$ $b = -0.00013^{+0.0154, +0.0308}_{-0.0155, -0.0305}$
w CDM	$a = -0.0168^{+0.0711, +0.1397}_{-0.0702, -0.1392}$ $b = -0.00015^{+0.0153, +0.0303}_{-0.0154, -0.0304}$
CPL	$a = -0.0183^{+0.0712, +0.14}_{-0.0711, -0.1401}$ $b = 0.00018^{+0.0159, +0.0306}_{-0.0155, -0.0301}$

with lensing, as well as WMAP polarization data at low multipoles with $l \leq 23$. The acoustic scale is

$$l_a = \pi \frac{\Omega_k^{-1/2} H_0^{-1} \text{sinn}[\Omega_k^{1/2} \int_0^{z_*} dz/E(z)]}{r_s(z_*)}, \quad (16)$$

where $r_s(z_*) = H_0^{-1} \int_{z_*}^\infty c_s(z)/E(z) dz$ is the comoving sound horizon at the recombination. The shift parameter is

$$R(z_*) = \frac{\sqrt{\Omega_m}}{\sqrt{|\Omega_k|}} \text{sinn} \left(\sqrt{|\Omega_k|} \int_0^{z_*} \frac{dz}{E(z)} \right). \quad (17)$$

The recombination redshift z_* is fitted by (Hu et al. 1996)

$$\begin{aligned} z_* &= 1048 [1 + 0.00124(\Omega_b h^2)^{-0.738}] [1 + g_1(\Omega_m h^2)^{g_2}], \\ g_1 &= \frac{0.0783(\Omega_b h^2)^{-0.238}}{1 + 39.5(\Omega_b h^2)^{0.763}}, \\ g_2 &= \frac{0.560}{1 + 21.1(\Omega_b h^2)^{1.81}}. \end{aligned} \quad (18)$$

The χ^2 value for the CMB data is

$$\chi_{\text{CMB}}^2 = \Delta \mathbf{P}_{\text{CMB}}^T \mathbf{C}_{\text{CMB}}^{-1} \Delta \mathbf{P}_{\text{CMB}}, \quad (19)$$

where $\Delta \mathbf{P}_{\text{CMB}} = \mathbf{P}_{\text{th}} - \mathbf{P}_{\text{obs}}$, \mathbf{P}_{obs} and \mathbf{P}_{th} are the observed and the theoretical values of the derived parameters, respectively, and \mathbf{C}_{CMB} is the covariance matrix for the derived CMB data (Wang et al. 2013).

4. CONSTRAINTS ON THE LIV PARAMETERS AND ANALYSIS

To explain the cosmic acceleration, an exotic energy component called dark energy with negative pressure was proposed (Riess et al. 1998; Perlmutter et al. 1999; Astier et al. 2006; Hicken et al. 2009; Amanullah et al. 2010; Spergel et al. 2003, 2007; Komatsu et al. 2009, 2011; Tegmark et al. 2004; Eisenstein et al. 2005; Cao et al. 2011, 2012a,b; Gao & Gong 2014; Gong et al. 2013, 2014). The most simple candidate for dark energy is the vacuum energy known as the cosmological constant Λ . Because of the huge difference between predicted and measured values of the vacuum energy, many other dynamical dark energy models have also been considered, including quintessence (Ratra et al. 1988; Caldwell et al. 1998), phantom (Caldwell et al. 2002, 2003), k-essence (Armendariz-Picon et al. 2001; Chiba et al. 2002), as well as quintom models (Feng et al. 2005, 2006; Guo et al. 2005). In this paper, we consider three

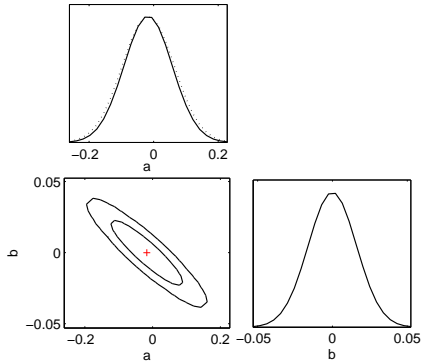


Figure 1. The marginalized 1σ and 2σ contours and the distribution of the LIV parameters for the Λ CDM model. The red cross represents the best-fit point.

different dark energy models: the Λ CDM model, the dark energy model with constant equation of state parameter w , and the Chevallier-Polarski-Linder (CPL) model (Chevallier et al. 2001; Linder et al. 2003).

For the Λ CDM model, the equation of state parameter $w = p/\rho = -1$ and the Friedmann equation is

$$h^2(z) = \Omega_m(1+z)^3 + \Omega_\Lambda, \quad (20)$$

where Ω_m is the matter energy density, and the dark energy density is Ω_Λ . Since $\Omega_m + \Omega_\Lambda = 1$ for a flat Λ CDM model, so we have only one independent parameter Ω_m in this model. By fitting the Λ CDM model to the above data, we get the 1σ and 2σ constraints: $a = -0.017^{+0.0717, +0.1416}_{-0.0718, -0.1415}$, $b = -0.00013^{+0.0154, +0.0308}_{-0.0155, -0.0305}$, $\Omega_m = 0.29^{+0.010, +0.022}_{-0.011, -0.022}$, and $H_0 = 69.5^{+0.9, +1.8}_{-0.9, -1.7}$. The results show that Lorentz invariance is consistent with the data. We show the results on a and b in Table 2. The 1D probability distribution of each parameter and the 2D confidence contours for the parameters are shown in Fig. 1.

For the flat w CDM model, the Friedmann equation is

$$h^2(z) = \Omega_m(1+z)^3 + \Omega_X(1+z)^{3(1+w)}, \quad (21)$$

where the dark energy density $\Omega_X = 1 - \Omega_m$. Using the MCMC method, the marginalized 1σ and 2σ constraints on the model parameters are: $a = -0.0168^{+0.0711, +0.1397}_{-0.0702, -0.1392}$, $b = -0.00015^{+0.0153, +0.0303}_{-0.0154, -0.0304}$, $\Omega_m = 0.288^{+0.011, +0.022}_{-0.011, -0.021}$, $w = -1.05^{+0.04, +0.079}_{-0.045, -0.088}$, and $H_0 = 70.2^{+1.1, +2.1}_{-1.1, -2.1}$. There is no evidence of LIV in w CDM model. The results are shown in Table 2, and the marginalized plots are shown in Fig. 2.

For the CPL model, the equation of state parameter is parameterized as $w(z) = w_0 + w_1 z/(1+z)$ and the Friedmann equation is

$$h^2(z) = \Omega_m(1+z)^3 + \Omega_X(1+z)^{3(1+w_0+w_1)} \exp\left(-\frac{3w_1 z}{1+z}\right). \quad (22)$$

In this model, Ω_m , w_0 , and w_1 are the model parameters. Fitting the CPL model to the combined data, we obtain the marginalized 1σ and 2σ constraints on the model parameters: $a = -0.0183^{+0.0712, +0.14}_{-0.0711, -0.1401}$, $b = 0.00018^{+0.0159, +0.0306}_{-0.0155, -0.0301}$, $\Omega_m = 0.288^{+0.012, +0.024}_{-0.012, -0.022}$,

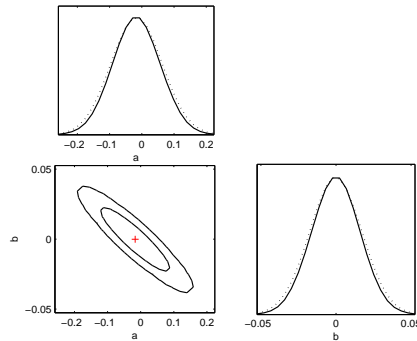


Figure 2. The marginalized 1σ and 2σ contours and the distribution of the LIV parameters for the w CDM model. The red cross represents the best-fit point.

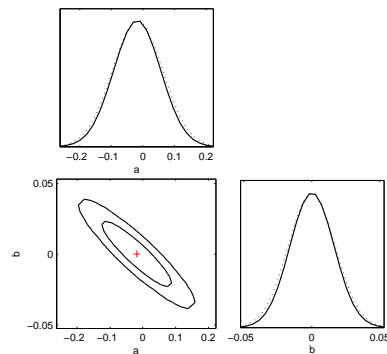


Figure 3. The marginalized 1σ and 2σ contours and the distribution of the LIV parameters for the CPL model. The red cross represents the best-fit point.

$w_0 = -1.02^{+0.123, +0.246}_{-0.122, -0.237}$, $w_1 = -0.203^{+0.593, +1.053}_{-0.595, -1.281}$, and $H_0 = 70.3^{+1.27, +2.45}_{-1.0, -2.57}$. We see no evidence of LIV in the CPL model. The constraints on a and b are shown in Table 2, the marginalized probability distributions and the 1σ and 2σ contours of a and b are shown in Fig. 3.

In the previous analysis, the model parameters take fixed values and a weak indication of LIV was found (Ellis et al. 2006; Biesiada et al. 2009). Here we consider the possible degeneracies among all the parameters and take all the parameters as free parameters, we find no evidence of LIV and all the results are consistent with each other. The conclusion is independent of the background model. Although the uncertainties on the parameters a and b become larger due to more fitting parameters, the difference on a for different cosmological model is still relatively small. To better understand the effect of the background model, we show the re-scaled spectral time lags $\Delta t_{obs}/(1+z)$ versus the $K(z)$ function for the three different cosmological models in Figs. 4-6, the data from GRBs is also shown in the figures. Because the background cosmological model changes the value of $K(z)$, so the value of a also changes. Unlike the models considered in Biesiada et al. (2009), the w CDM model and CPL model considered here is close to the Λ CDM model as seen from the above best-fitting values of w , w_0

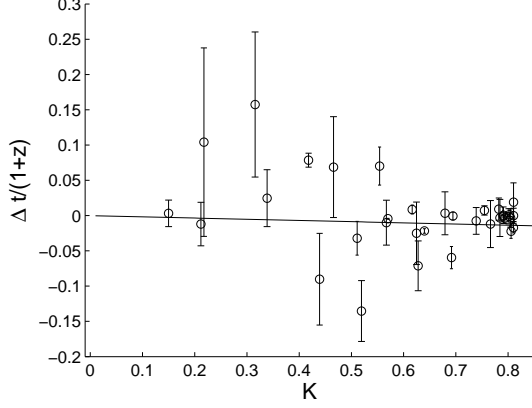


Figure 4. The re-scaled spectral time-lags $\Delta t_{obs}/(1+z)$ versus $K(z)$ for the Λ CDM model with $\Omega_m = 0.29$. The solid line represents the best fit with the linear regression.

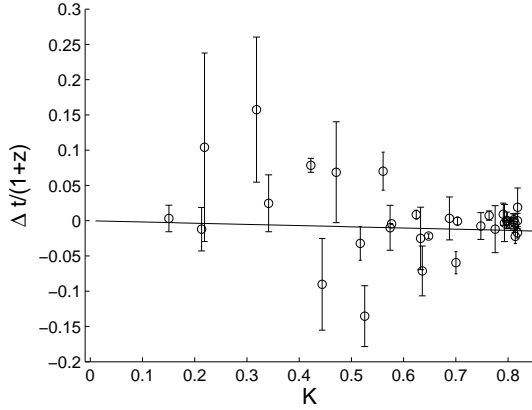


Figure 5. The re-scaled spectral time-lags $\Delta t_{obs}/(1+z)$ versus $K(z)$ for the w CDM model with $\Omega_m = 0.288$ and $w = -1.05$. The solid line represents the best fit with the linear regression.

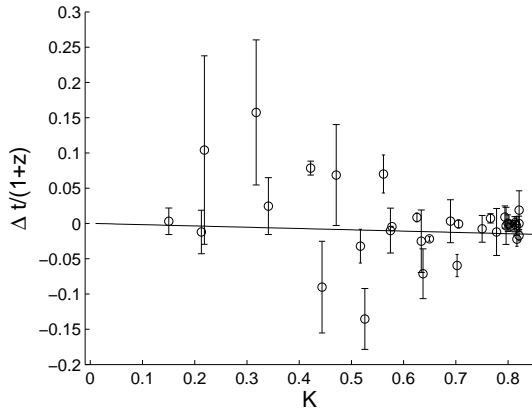


Figure 6. The re-scaled spectral time-lags $\Delta t_{obs}/(1+z)$ versus $K(z)$ for the CPL model with $\Omega_m = 0.288$, $w_0 = -1.02$ and $w_1 = -0.203$.

and w_1 , so our results are all consist with each other.

The redshifts of the GRBs span from $z = 0.168$ to $z = 6.29$, so we also consider the effect of the redshift

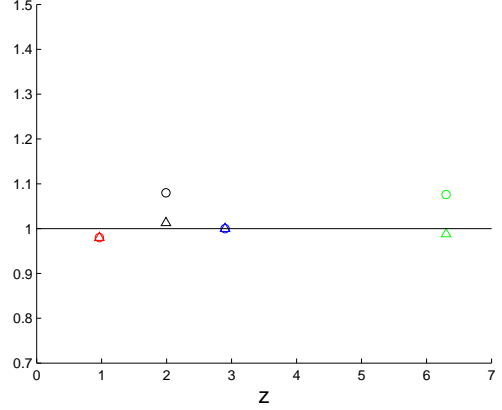


Figure 7. The constraint on the slope a for the w CDM and CPL models normalized to Λ CDM model by using four sub-samples of GRBs. The GRBs are divided into 4 groups with upper boundaries at $z = 1.0$, $z = 2.0$, $z = 3.0$ and $z = 6.3$. The circles represent the CPL model and the triangles are for w CDM model. The red, black, blue and green are for the fits to data with redshifts $z < 1$, $z < 2$, $z < 3$ and $z > 3$, respectively.

distribution on the results. We divide the GRBs into 4 groups with upper boundaries at $z = 1.0$, $z = 2.0$, $z = 3.0$ and $z = 6.3$. The first group has 11 GRBs with redshifts $0 < z < 1.0$, the second group has 21 GRBs with redshifts $0 < z < 2.0$, the third group has 27 GRBs with redshifts $z < 3.0$ and the fourth group contains all 35 GRBs. We then fit the cosmological models to each group of GRBs, and the constraints on the slope a normalized to the Λ CDM model are shown in Fig. 7. The difference between different models are negligible in the first and the third redshift groups. For both w CDM and the CPL models, the effects of redshift distributions are similar although the deviation is a little larger for the CPL model. The biggest contribution comes from the GRBs with redshifts in the range $1 < z < 2$ and $z > 3$. As we discussed above, the CPL model deviates more from Λ CDM than w CDM model does, so the value of the slope a for the Λ CDM model is more negative. The reason of the redshift-dependence is due to distributions of the GRBs. In the first and third groups, the average of the spectral time lags is close to zero. But we have more negative Δt data in the redshift intervals $1 < z < 2$ and $z > 3$, therefore we see bigger deviations for the data up to redshift 2 and for the whole data.

5. CONCLUSIONS

We test the LIV with the 35 GRBs, the Union2 SNeIa, the CMB and BAO data for three different cosmological models. The slope a and the intercept b in the linear regression method as well as the model parameters are fitted to the combined data. For the Λ CDM model, the marginalized 1σ and 2σ results are: $a = -0.017^{+0.0717, +0.1416}_{-0.0718, -0.1415}$, and $b = -0.00013^{+0.0154, +0.0308}_{-0.0155, -0.0305}$. For the w CDM model, the marginalized 1σ and 2σ results are: $a = -0.0168^{+0.0711, +0.1397}_{-0.0702, -0.1392}$, and $b = -0.00015^{+0.0153, +0.0303}_{-0.0154, -0.0304}$. For the CPL model, we obtain the marginalized 1σ and 2σ results $a = -0.0183^{+0.0712, +0.14}_{-0.0711, -0.1401}$, and $b = 0.00018^{+0.0159, +0.0306}_{-0.0155, -0.0301}$. These results are also summarized in Table 2. Because the slope a is consistent with $a = 0$ for all the three mod-

els, there is no evidence of LIV. The results for all the three models are also consistent. Our conclusion is in conflict with previous result by Biesiada et al. (2009). In their studies, the model parameters are fixed at certain values, so the degeneracies among parameters are neglected. The dynamical dark energy models with the fixed parameter values discussed in the previous work are very different from Λ CDM model, so they found different results for different cosmological models. In our analysis, we treat the model parameters as free parameters, and the model parameters are fitted with the latest SNeIa and BAO data. The best fitted w CDM and CPL models are close to Λ CDM model. Although the uncertainties on the model parameters become almost double compared with the previous analysis (Biesiada et al. 2009) due to more fitting parameters, the differences between different model are relatively small and all the results are consistent. Because the GRBs' data is not uniformly distributed, especially in the redshift intervals $1 < z < 2$ and $z > 3$, we see the small differences between different models come from the GRBs at the redshift intervals $1 < z < 2$ and $z > 3$. In conclusion, our results show no evidence of LIV in the three cosmological models.

The results are also in good agreement with the recent neutrino analysis, which discussed LIV using two cascade neutrino events with energies around 1 PeV recently detected by IceCube Borriello et al. (2013). Yet it is worth noting that experimental probes of LIV are limited by the scarcity of GRB data. Other high-energy astrophysics experiments such as the photon time-delay measurements from objects like Pulsars (Kaaret et al. 1999) and Active Galactic Nuclei (AGN) (Albert et al. 2008) may provide complementary probe of LIV effect. Further studies are still needed to draw a more quantitative conclusion.

ACKNOWLEDGMENTS

This work was supported by the Ministry of Science and Technology National Basic Science Program (Project 973) under Grants Nos. 2012CB821804 and 2014CB845806, the National Natural Science Foundation of China under Grants Nos. 11073005, 11373014 and 11447213, the Fundamental Research Funds for the Central Universities and Scientific Research Foundation of Beijing Normal University, and China Postdoctoral Science Foundation under Grant No. 2014M550642. Y.G. is supported by the National Natural Science Foundation of China under grant Nos. 11175270 and 11475065, and the Program for New Century Excellent Talents in University under grant No. NCET-12-0205. This work was also supported by Scientific and Technological Research Program of Chongqing Municipal Education Commission (Grant No. KJ130535), the Scientific Research Foundation For Doctor of Chongqing University of Posts and Telecommunications (A2013-25), HG acknowledges NASA NNX 13AH50G .

REFERENCES

- Abdo, A. A. et al 2009, Nature 462, 331-334
 Abdo, A. A. et al 2009, Science 323, 1688-1693
 Ade, P. et al. 2014, A&A, 571, A16
 Albert, J. et al. 2008, PLB, 668, 253
 Amanullah, R. et al. 2010, ApJ, 716, 712
 Amelino-Camelia, G. et al. 1998, Nature, 393, 763
 Amelino-Camelia, G. et al. 2001, PRD, 64, 036005
 Amelino-Camelia, G. et al. 2002, Int. J. Mod. Phys. D, 11, 35-60
 Amelino-Camelia, G. et al. 2009, PRL, 103, 171302
 Amelino-Camelia, G. 2013, Living Rev. Rel, 16, 5
 Armendariz-Picon, C. et al. 2001, PRD, 63, 103510
 Astier, P. et al. 2006, A&A, 447, 31
 Baukh, V. et al. 2007, PRD, 76, 027502
 Beutler, F. et al. 2011, 416, 3017
 Biesiada, M. et al. 2007, JCAP, 0705, 011
 Biesiada, M. et al. 2009, Class. Quantum Gravity, 26, 125007
 Biller, S. D. et al. 1999, PRL, 83, 2108
 Blake, C. et al. 2011, MNRAS, 418, 1707
 Borriello, E. et al. 2013, PRD, 87, 116009
 Caldwell, R. R. et al. 1998, PRL, 80, 1582
 Caldwell, R. R. et al. 2002, PLB, 545, 23
 Caldwell, R. R. et al. 2003, PRL, 91, 071301
 Cao, S. et al. 2011, Science in China G: Physics and Astronomy, 54, 2260
 Cao, S. et al. 2012a, JCAP, 1203, 016
 Cao, S. et al. 2012b, ApJ, 755, 31
 Chevallier, M. et al. 2001, IJMPD, 10, 213
 Chiba, T. et al. 2002, PRD, 66, 063514
 Eisenstein, D. J. et al. 1998, ApJ, 496, 605
 Eisenstein, D. J. et al. 2005, ApJ, 633, 560
 Ellis, J. et al. 2003, A&A, 402, 409
 Ellis, J. et al. 2006, Astroparticle Physics, 25, 402; 29, 158 (E)
 Ellis, J. et al. 2008, A&A, 402, 409
 Feng, B. et al. 2005a, PLB, 607, 35
 Feng, B. et al. 2006, PLB, 634, 101
 Gao, Q., & Gong, Y. 2014, Class. Quantum Gravity, 31, 105007
 Gong, Y. et al. 2013, MNRAS, 430, 3142
 Gong, Y. et al. 2014, Eur. Phys. J. C, 74, 2729
 Guo, Z.-K. et al. 2005, PLB, 608, 177
 Hicken, M. et al. 2009, ApJ, 700, 1097
 Hu, W. et al. 1996, ApJ, 471, 542
 Jacob, U. et al. 2007, Nature Physics, 3, 87
 Jacob, U. et al. 2008, JCAP, 0801, 031
 Kaaret, P. et al. 1999, A&A, 345, L32
 Komatsu, E. et al. 2009, ApJS, 180, 330
 Komatsu, E. et al. 2011, ApJS, 192, 18
 Kowalski-Glikman, J., & Nowak, S. 2002, Phys.Lett. B, 539, 126-132
 Lewis, A. et al. 2002, PRD, 66, 103511
 Linder, E. V. et al. 2003, PRD, 68, 083504
 Mattingly, D. et al. 2005, Living Reviews in Relativity, 8, 5
 Percival, W. J. et al. 2010, MNRAS, 401, 2148
 Perlmutter, S. et al. 1999, ApJ, 517, 565
 Ratra, B. et al. 1988, PRD, 37, 3406
 Riess, A. G. et al. 1998, AJ, 116, 1009
 Rodriguez Martínez, M., & Piran, T. 2006, JCAP, 0604, 006
 Sarkar, S. et al. 2002, MPLA, 17, 1025
 Spergel, D. N. et al. 2003, ApJS, 148, 175
 Spergel, D. N. et al. 2007, ApJS, 170, 377
 Tegmark, M. et al. 2004, ApJ, 606, 702
 Wang, Y. et al. 2013, PRD, 88, 043522